Multiple representations of the body schema for the same body part

Kazumichi Matsumiya[a,b,1]

[a]Graduate School of Information Sciences, Tohoku University, Sendai 980-8579, Japan; and [b]Japan Science and Technology Agency, Precursory Research for Embryonic Science and Technology, Sendai 980-8579, Japan

Edited by Ranulfo Romo, Instituto de Fisiologia Celular, Universidad Nacional Autonoma de Mexico, Mexico City, Mexico; received July 5, 2021; accepted December 1, 2021

Purposeful motor actions depend on the brain's representation of the body, called the body schema, and disorders of the body schema have been reported to show motor deficits. The body schema has been assumed for almost a century to be a common body representation supporting all types of motor actions, and previous studies have considered only a single motor action. Although we often execute multiple motor actions, how the body schema operates during such actions is unknown. To address this issue, I developed a technique to measure the body schema during multiple motor actions. Participants made simultaneous eye and reach movements to the same location of 10 landmarks on their hand. By analyzing the internal configuration of the locations of these points for each of the eye and reach movements, I produced maps of the mental representation of hand shape. Despite these two movements being simultaneously directed to the same bodily location, the resulting hand map (i.e., a part of the body schema) was much more distorted for reach movements than for eye movements. Furthermore, the weighting of visual and proprioceptive bodily cues to build up this part of the body schema differed for each effector. These results demonstrate that the body schema is organized as multiple effector-specific body representations. I propose that the choice of effector toward one's body can determine which body representation in the brain is observed and that this visualization approach may offer a new way to understand patients' body schema.

body representation | eye movements | hand movements | motor actions | multisensory integration

Since a classic work of Head and Holmes in the early 1900s (1), it has been widely accepted that purposeful motor actions rely on a spatial representation of the body in the brain, called the body schema (2–6). Without the body schema, we would be unable to accurately and safely control our body parts. Indeed, impairment of the body schema leads to a variety of disorders ranging from motor dysfunction to delusions that the affected body part belongs to another person (7, 8). The classic notion of the body schema had long been used to describe a representation of the location of body parts in external space derived from information about body posture specified by afferent signals (i.e., proprioceptive signals) and from information about efferent copies of motor commands (9–11). However, current views on the body schema suggest that the ability to localize body parts in external space requires not only afferent and efferent information but also stored information about the body's metric properties, such as body part size and shape, because no afferent and efferent signals directly inform the brain about the metric properties of body parts (12, 13). This stored body metric information is provided by an implicit body representation in the brain (12). Such a metric representation serves not only perception but also action (13). Based on the current views, the body schema can be defined as a representation of the location of body parts in space that is constructed by combining afferent and efferent information with stored information about the body metrics. Moreover, the body schema has been suggested to be involved in a global adjustment through afferent signals from various body parts (14). Indeed, afferent signals coming from all body parts, such as the eye and foot, function together in modulating motor control (15, 16). Taken together, the body schema contains the spatial configuration of the body used for the guidance of action and functions in a global way.

The accumulated research literature indicates that the body schema is constructed based on bodily signals from multiple sensory sources such as vision and proprioception (5, 6, 17–20). The spatial and temporal congruence of multisensory bodily signals from one's body parts generates a single estimate of the body's location (21–26). This is referred to as multisensory integration (27–29). The process underlying multisensory integration determines how much a given sensory modality contributes to the final estimate relative to a different sensory modality in a statistically optimal way (30–32). Supporting this multisensory integration model, many demonstrations show that the weighting of each sensory source of bodily signals varies with its reliability (33–35). The importance of multisensory integration for the body schema is illustrated in a cross-modal effect in which the position sense of one's hand is influenced by vision of an artificial hand (36).

The body schema is normally assumed to be a common body representation supporting all types of motor actions, and numerous studies have typically used a single motor task to explore aspects of the body schema (17, 19, 37–40). However, we often take multiple simultaneous actions with different effectors, such as the eye and hand, in our daily lives. In recent

Significance

Accurate motor control depends on maps of the body in the brain, called the body schema. Disorders of the body schema cause motor deficits. Although we often execute actions with different motor systems such as the eye and hand, how the body schema operates during such actions is unknown. In this study, participants simultaneously directed eye and hand movements to the same body part. These two movements were found to be guided by different body maps. This finding demonstrates multiple motor system–specific representations of the body schema, suggesting that the choice of motor system toward one's body can determine which of the brain's body maps is observed. This may offer a new way to visualize patients' body schema.

Author contributions: K.M. designed research, performed research, analyzed data, and wrote the paper.

The author declares no competing interest.

This article is a PNAS Direct Submission.

[1]Email: matsumiya@tohoku.ac.jp.

This article contains supporting information online at http://www.pnas.org/lookup/suppl/doi:10.1073/pnas.2112318119/-/DCSupplemental.

Published January 19, 2022.

years, growing evidence has indicated that, when multiple actions are performed with different types of effectors, the action for each effector is guided by a different spatial representation of the outside world in the brain, such as motor responses to visual motion (41), localization of moving objects (42), and allocation of spatial attention (43, 44). These results suggest that there are multiple spatial maps of the outside world in the brain and that each of these spatial maps guides a different effector. This is surprising because it is thought that the spatial maps are represented in a common reference frame (i.e., eye-centered coordinates) regardless of whether the action is an eye movement or a reach movement (45–50). However, how the body schema operates during multiple actions with different effectors is unknown. Here, I systematically investigate the body schema mediating the spatial configuration of the hand when simultaneous eye and reach movements are made to that hand. The present results demonstrate that the body schema is organized as multiple effector-specific representations of the body.

The body schema contributes to the planning of motor actions toward one's body parts. It seems natural that the planning of motor actions toward one's body parts would use the same bodily information that allows us to perceive those body parts. However, bodily information has been suggested to undergo independent processing when used for ballistic motor responses as opposed to perceptual judgments (19, 51). Based on this finding, I developed a technique to measure the body schema during multiple motor actions by having participants make ballistic motor responses toward landmarks on a hand. The distance between the judged locations of two adjacent landmarks on the hand (e.g., the tip and knuckle of a single finger) depends only on the represented length of the body segment connecting them. Other sources of error, such as misjudgments of the knuckle angle, affect localization error for a single landmark (e.g., the distance between actual and judged locations at the tip of the finger) but preserve the relative positions of the landmarks. Thus, the body schema was isolated and measured by having participants make simultaneous eye and reach movements toward the location of 10 landmarks on their hand. By comparing the landing positions of eye and reach at these landmarks regardless of their true positions (Fig. 1*C*), I analyzed the internal spatial configuration of the hand representations for the eye and reach landing positions. The distances between these motor judgments for each effector are different from either constant or variable error of localization and allow me to estimate the internal structural representation of the body schema of the hand. This behavioral measurement of the body schema was combined with the cross-modal effect of a computer-generated hand on proprioceptive judgments (36). By using this effect, I was able to investigate whether the weighting of visual and proprioceptive cues to the location of the landmarks differed between eye and reach landing positions.

Results

Experiment 1: With Vision of a Hand. Participants placed their right hand palm down under a transparent board and wore a head-mounted display (HMD) that displayed visual stimuli in stereoscopic three dimensions (3D) (Fig. 1*A*). The HMD showed a realistic life-sized computer graphics (CG) hand (Fig. 1*D*). The CG hand overlapped the participant's unseen right hand in the virtual environment and was configured similarly to the participant's actual hand. While participants viewed the CG hand, they made simultaneous eye and reach (left forefinger) movements toward the location of 10 landmarks on their hidden right hand (the knuckles and tips of each finger). In such coordinated eye and reach movements, eye movement onset preceded hand movement onset (Fig. 1*B*; see *SI Appendix*, Fig. S1 for more details), as confirmed by previous studies (52–54). Based on a previous study (12), comparing the eye or reach landing position of different landmarks allowed me to build a spatial map of the mental representation of hand shape (i.e., hand map), which could be then compared with the actual hand shape. Fig. 1*C* shows an example: The targeted locations of the index fingertip and knuckle were used to calculate the represented index finger length (dotted red line) for comparison with its actual length (dotted black line). Before and after

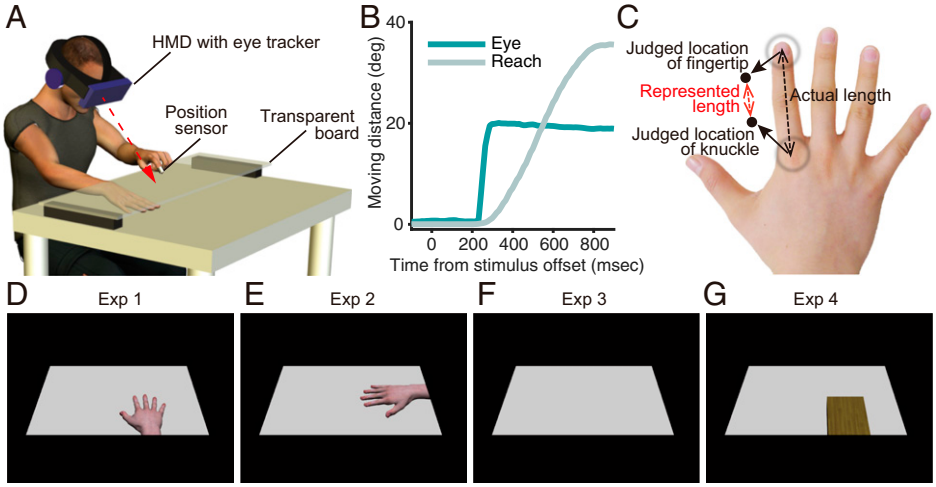

Fig. 1. Experimental setups. (*A*) Participants binocularly viewed the visual stimuli presented through an HMD with an eye tracker and placed their right hand on a table. A transparent board was placed over the participant's right hand. A position sensor was attached to the tip of the participant's left index finger. (*B*) Sample result of eye and reach movements for one participant. (*C*) The represented length of a finger was determined by comparing the distance between the judged positions of the fingertip and knuckle without respect to their true positions. This distance was then compared with the true finger length. Thus, the represented hand shape was assessed by examining the internal configuration of the localizations of multiple landmarks. (*D*–*G*) Visual stimuli. (*D*) A CG hand was presented on a gray surface in the virtual environment, and the CG hand was placed so that it overlapped the participant's unseen right hand (experiment 1). (*E*) The CG hand and the participant's unseen right hand were rotated 90° so that their fingers pointed to the left (experiment 2). (*F*) The CG hand was not presented in the virtual environment, but the participant's unseen right hand was placed on the gray surface as in experiment 1 (experiment 3). (*G*) A wood-like rectangle was presented on the gray surface instead of the CG hand, and the rectangle was placed so that it overlapped the participant's unseen right hand, as in experiment 1 (experiment 4).

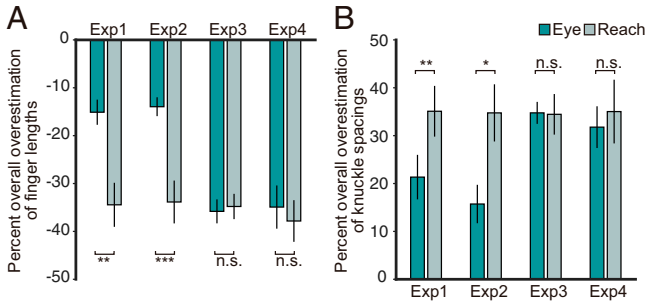

Fig. 2. Percent overall overestimation of finger lengths and spacing between knuckles for experiments 1 through 4. (*A*) Finger lengths. The distance between the landing locations of each knuckle and fingertip was calculated to estimate the represented finger length, and the estimated finger length was averaged from the thumb to the little finger. (*B*) Knuckle spacings. The distance between pairs of adjacent knuckles was calculated as for finger length, and the estimated knuckle spacing was averaged among the index–thumb, the middle–index, the ring–middle, the little–ring, and the index–little knuckles. The dark green and light green symbols represent eye and reach movements, respectively. Results are the mean ± SE. $*P < 0.05$; $**P < 0.01$; $***P < 0.005$; n.s.: not significant.

each block, a picture was taken to record the actual hand shape and to ensure that the hand had not moved.

To assess finger length, the distance between the average landing positions of each knuckle and fingertip was calculated from the thumb to the little finger. These distances were then averaged to estimate overall finger length. The estimated overall finger length underestimated the actual length for both eye and reach landing positions [t (11) = −5.75, $P < 0.001$, and t (11) = −7.49, $P < 0.0001$, respectively; Fig. 2*A*; see *SI Appendix*, Fig. S2 for more details], which is consistent with the results of the previous study (12). Intriguingly, the overall underestimation of finger length significantly differed between the eye and reach landing positions [paired t test, t (11) = 4.39, $P < 0.01$; Fig. 2*A*].

To assess hand width, the distance between pairs of adjacent knuckles was calculated as for finger length. These distances were then averaged to estimate overall knuckle spacing. In contrast to the overall underestimation of finger length, strong overall overestimation of knuckle spacing was observed [t (11) = 4.59, $P < 0.001$, for eye landing positions and t (11) = 6.62, $P < 0.0001$, for reach landing positions; Fig. 2*B*; see *SI Appendix*, Fig. S2 for more details], which is consistent with the results of previous work (12). Overall overestimation of knuckle spacing significantly differed between the eye and reach landing positions [paired t test, t (11) = −3.14, $P < 0.01$; Fig. 2*B*].

To assess the shape of the hand map in detail, generalized Procrustes superimposition (GPS) (55) was used to compare the actual configuration of landmarks from each participant's right hand with the internal representation based on eye and reach landing positions (Fig. 3 *A* and *B*). GPS removes differences in location, rotation, and scale and thereby highlights differences in shape (55, 56). Analysis of these data indicated significant differences in mean shape between the actual hand and the resulting hand map for eye landing positions [Bonferroni-corrected Goodall's F test: Goodall's $F(16, 352) = 5.50$, $P < 0.0001$; Fig. 3*A*; see *SI Appendix, SI Materials and Methods* for further details] and reach landing positions [Goodall's $F(16, 352) = 17.75$, $P < 0.0001$; Fig. 3*B*]. Although the shape of the hand map was distorted for both eye and reach landing positions, the shape was more similar to the actual shape of the hand in eye landing positions than in reach landing positions. The mean shape of the hand map significantly differed between eye and reach landing positions [Goodall's $F(16, 352) = 5.56$, $P < 0.0001$].

One might argue that the difference in measured positions between eye and reach movements might reflect differential times of motor actions, rather than the difference in body representations, because eye and reach movements do not have the same speed or the same landing time (see *SI Appendix, SI Results* for details; *SI Appendix*, Fig. S3). However, this is unlikely. The initial movement end point was used to calculate the landing positions of the movement for each of the eye and reach movements. Moreover, I confirmed that there were significant differences in the overestimation of finger lengths and knuckle spacings between eye and reach, even though reach movements had latencies comparable to those of eye movements (see *SI Appendix, SI Results* for details; *SI Appendix*, Fig. S4). Thus, the difference in measured positions between eye and reach reflects a difference in the spatial representations of the body rather than the differential starting times of motor actions.

Experiment 2: Rotated Posture. The results of experiment 1 could potentially reflect either a foreshortening of perspective in the near–far axis or motor biases in trunk-based coordinates for motor responses. To address these issues, a second experiment was conducted in which participants' hands and the CG hand were rotated 90° counterclockwise relative to their trunk so that the fingers were pointing toward the left (Fig. 1*E*). If any

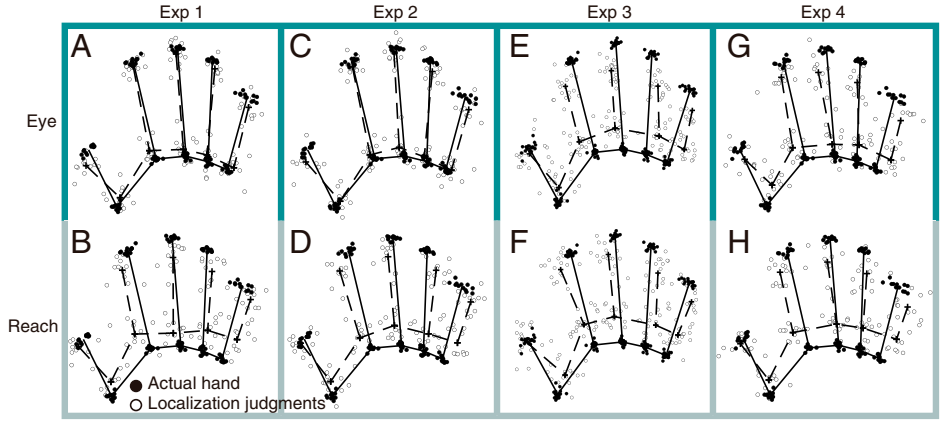

Fig. 3. GPS of landmark positions for actual hands (black dots/solid lines) and the represented hand shape inferred from eye and reach movements (white dots/dotted lines). The solid line indicates the mean shape of the actual hand. The dotted line indicates the mean shape of the represented hand shape. (*A* and *B*) Experiment 1, (*C* and *D*) experiment 2, (*E* and *F*) experiment 3, and (*G* and *H*) experiment 4. The dark green and light green frames represent eye and reach movements, respectively.

effects independent of the hand map reproduce the results of experiment 1, these effects should be reversed in the rotated posture relative to the original posture used in experiment 1 (i.e., the fingers pointing away from the trunk): extended finger lengths and narrow hand widths. However, experiment 2 showed almost identical estimated finger lengths and hand widths in the rotated posture to those in the original posture. Finger length was underestimated overall even in the rotated posture [t (11) = −7.08, $P < 0.0001$, for eye landing positions and t (11) = −7.57, $P < 0.0001$, for reach landing positions; Fig. 2*A*; see *SI Appendix*, Fig. S2 for more details] and significantly differed between eye and reach landing positions [paired t test, t (11) = 4.64, $P < 0.001$; Fig. 2*A*]. Knuckle spacing was overestimated overall [t (11) = 3.92, $P < 0.01$, for eye landing positions and t (11) = 5.82, $P < 0.001$, for reach landing positions; Fig. 2*B*; see *SI Appendix*, Fig. S2 for more details] and significantly differed between eye and reach landing positions [paired t test, t (11) = −2.41, $P < 0.05$; Fig. 2*B*]. Analysis of GPS data revealed significant differences in the mean shape between the actual hand and the resulting hand map for eye landing positions [Goodall's F(16, 352) = 4.57, $P < 0.0001$; Fig. 3*C*] and reach landing positions [Goodall's F(16, 352) = 16.88, $P < 0.0001$; Fig. 3*D*]. As in experiment 1, the shape of the hand map was more similar to the actual shape of the hand in eye landing positions than in reach landing positions. The mean shape of the hand map significantly differed between eye and reach landing positions [Goodall's F(16, 352) = 5.97, $P < 0.0001$]. Thus, these results demonstrate that the effects observed in the present study reflect the hand map in the brain rather than biases in head- or trunk-based coordinates for motor responses or in a foreshortening of perspective in the near–far axis.

Experiment 3: Without Vision of a Hand. To investigate whether viewing a hand affected the shape of the hand map in experiments 1 and 2, the CG hand was not presented to participants and they were asked to make concurrent eye and reach movements to the location of 10 landmarks on their hidden right hand (Fig. 1*F*). Under these conditions, finger length was underestimated overall [t (17) = −17.36, $P < 0.0001$, for eye landing positions and t (17) = −16.06, $P < 0.0001$, for reach landing positions; Fig. 2*A*; see *SI Appendix*, Fig. S2 for more details] but was not significantly different between eye and reach landing positions [paired t test, t (17) = −0.30, $P = 0.76$; Fig. 2*A*]. Knuckle spacing was overestimated overall [t (17) = 15.13, $P < 0.0001$, for eye landing positions and t (17) = 8.13, $P < 0.0001$, for reach landing positions; Fig. 2*B*; see *SI Appendix*, Fig. S2 for more details] but was not significantly different between eye and reach landing positions [paired t test, t (17) = 0.058, $P = 0.95$; Fig. 2*B*]. Analysis of GPS data revealed significant differences in the mean shape between the actual hand and the hand map for eye landing positions [Goodall's F(16, 544) = 47.28, $P < 0.0001$; Fig. 3*E*] and reach landing positions [Goodall's F(16, 544) = 25.21, $P < 0.0001$; Fig. 3*F*]. However, there was no significant difference in the mean shape of the hand map between eye and reach landing positions [Goodall's F(16, 544) = 1.22, $P = 0.25$]. These results indicate that hand viewing is required to generate the difference in the shape of the hand map between eye and reach landing positions.

Experiment 4: With a Wood-Like Rectangle. To investigate whether the difference in the shape of the hand map between eye and reach movements is specific to vision of a hand, the CG hand was visually replaced with a computer-generated wood-like rectangle that spatially overlapped the participant's unseen right hand, as in experiment 1 (Fig. 1*G*). Finger length was underestimated overall [t (11) = −7.74, $P < 0.0001$, for eye landing positions and t (11) = −8.70, $P < 0.0001$, for reach landing positions; Fig. 2*A*; see *SI Appendix*, Fig. S2 for more details] but was not significantly different between eye and reach landing positions [paired t test, t (11) = 1.37, $P = 0.20$; Fig. 2*A*]. Knuckle spacing was overestimated overall [t (11) = 7.29, $P < 0.0001$, for eye landing positions and t (11) = 5.26, $P < 0.001$, for reach landing positions; Fig. 2*B*; see *SI Appendix*, Fig. S2 for more details] but was not significantly different between eye and reach landing positions [paired t test, t (11) = −0.48, $P = 0.64$; Fig. 2*B*]. Analysis of GPS data identified significant differences in the mean shape between the actual hand and the hand map for eye landing positions [Goodall's F(16, 352) = 11.96, $P < 0.0001$; Fig. 3*G*] and reach landing positions [Goodall's F(16, 352) = 18.59, $P < 0.0001$; Fig. 3*H*]. However, there was no significant difference in the mean shape of the hand map between eye and reach landing positions [Goodall's F(16, 352) = 1.29, $P = 0.20$]. These results indicate that the difference in the shape of the hand map between eye and reach movements is specific to vision of a hand.

Finger Lengths and Knuckle Spacings for Eye and Reach Are Different in Relation to Perception. Since separate somatosensory processes have been proposed for action and perception (51), I investigated whether the finger lengths and knuckle spacings for eye and reach are different from those for perception. Participants were instructed to judge the location of landmarks on their invisible right hand by moving a visual pointer in the virtual environment with a trackball controlled by their left hand (perceptual localization task; *SI Appendix, SI Materials and Methods*). In the "with CG hand" condition, the participants saw the CG hand, as in experiment 1. In the "without CG hand" condition, they saw a gray surface alone without the CG hand, as in experiment 3. I found that the finger lengths and knuckle spacings for reach differed from those for perception [Bonferroni-corrected paired t tests, t (11) = 5.23, $P < 0.01$, for finger lengths and t (11) = 2.71, $P < 0.05$, for knuckle spacings; Fig. 4 *A* and *B*; see *SI Appendix, SI Materials and Methods* and *SI Results* for details; *SI Appendix*, Fig. S5). In contrast, the finger lengths and knuckle spacings for eye were almost the same as those for perception [t (11) = 2.13, $P = 0.11$, for finger lengths and t (11) = 0.65, $P = 0.99$, for knuckle spacings; Fig. 4 *A* and *B*; see *SI Appendix, SI Results* for details; *SI Appendix*, Fig. S5]. Furthermore, participants answered questionnaire items to rate perceptual aspects of the CG hand (ownership rating task; see *SI Appendix, SI Materials and Methods*, Table S1, and *SI Results* for details; *SI Appendix*, Fig. S6) (25, 26, 35, 57). I found that the overestimation of the finger lengths and knuckle spacings was significantly correlated with the strength of sense of body ownership over the CG hand for eye and percept but not for reach (Fig. 4 *C–H*; see *SI Appendix, SI Materials and Methods* and *SI Results* for details). Note that it is suggested later that a different hand representation is used for eye movements and perception (see *Correlations across Individuals between Hand Maps*). Thus, these results point to a difference in the body map used to guide reach movements as opposed to that used to guide saccadic eye movements.

Hand Maps for Eye and Reach Are Different from the Conscious Body Image. To investigate whether the hand maps for eye and reach are dissociated from a conscious body image, I used Napier's shape index, which quantifies the ratio of hand width to length (58) (template-matching task; *SI Appendix, SI Materials and Methods*). I found differences in shape indices between the hand map for eye and the conscious body image and between the hand map for reach and the conscious body image [Bonferroni-corrected paired t tests, t (11) = 4.19, $P < 0.01$, for eye and t (11) = 5.55, $P < 0.005$, for reach; Fig. 5*A*; see *SI Appendix, SI Results* for details; *SI Appendix*, Fig. S7]. There was a significant difference in shape indices between eye and reach [t (11) = 3.38, $P < 0.05$; Fig. 5*A*]. Given that the hand maps for eye and

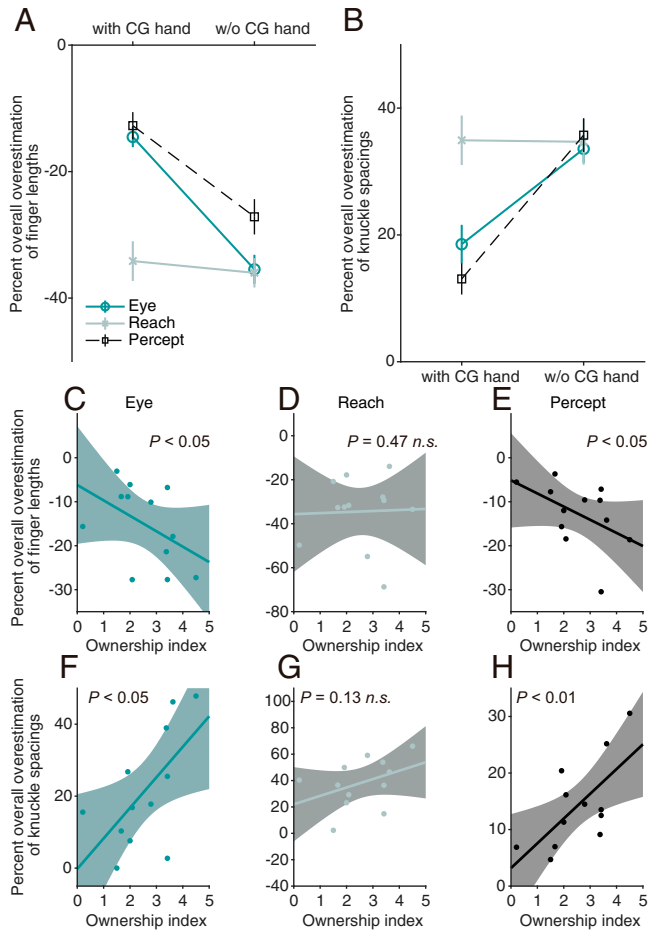

Fig. 4. Comparison of finger lengths and knuckle spacings among eye, reach, and percept. (*A*) Percent overall overestimation of finger lengths for the "with CG hand" and "without CG hand" conditions. (*B*) Percent overall overestimation of knuckle spacings for the "with CG hand" and "without CG hand" conditions. The dark green, light green, and dotted black lines represent eye, reach, and percept, respectively. Results are the mean ± SE. (*C–H*) Regression plot (and 95% confidence bands) of the strength of the sense of body ownership and overestimation of finger lengths and knuckle spacings for the "with CG hand" condition. (*C–E*) Percent overall overestimation of finger lengths for eye, reach, and percept. (*F–H*) Percent overall overestimation of knuckle spacings for eye, reach, and percept. *n.s.*: not significant.

reach were also different in relation to sense of body ownership as shown in Fig. 4 *C–H*, this sense of body ownership might involve the conscious body image (19, 59). However, I found no correlation between the shape and ownership indexes (*SI Appendix*, Fig. S8), implying that measures based on sense of body ownership may not be measures of body image.

Correlations across Individuals between Hand Maps. To determine whether a different hand representation is used between eye and reach, I analyzed the correlation across individuals between the shape indices, rather than the overestimation of finger lengths and knuckle spacings, for different effectors. The shape index is a better measure of the hand representation, because the overestimation of finger lengths and knuckle spacings shows the extent of distortion but does not represent the shape of the hand map itself. If the same hand representation is used between different effectors, there should be a correlation across individuals between the shape indices for these effectors (60). However, I found that there were no significant correlations between eye and reach under both the "with CG hand" and "without CG hand" conditions ($r_s = 0.16$, $n = 24$, and $P = 0.46$ for the "with CG hand" condition and $r_s = 0.20$, $n = 30$, and $P = 0.30$ for the "without CG hand" condition; see Fig. 5*B* and *SI Appendix*, Fig. S9 *A–D* and *SI Results* for details). In particular, I found no significant correlation between the shape indices for eye and reach movements without the CG hand (Fig. 5*B*), even though the average distortions of the hand map were similar between eye and reach without the CG hand (*SI Appendix*, Fig. S9*C*). Thus, these results suggest that different hand representations are used for eye and reach movements regardless of whether visual information about the hand is available. On the other hand, there was a significant correlation between the normal (experiment 1) and rotated (experiment 2) postures for each of eye and reach ($r_s = 0.68$, $n = 12$, and $P < 0.05$ for eye and $r_s = 0.81$, $n = 12$, and $P < 0.001$ for reach; see *SI Appendix*, Fig. S9 *E–H* and *SI Results* for details), suggesting that the same hand representation is used for the normal and rotated postures in the same effector. Furthermore, I found that there was no significant correlation between eye movements and perception ($r_s = -0.28$, $n = 12$, and $P = 0.38$; Fig. 5*C*; see *SI Appendix*, Fig. S9 *I* and *J* and *SI Results* for details), suggesting that different hand representations are used even for eye movements and perception. This implies that the distortions of hand shape in eye movements are not indicative of distortions in the perceptual body image.

Discussion

The present study reveals that there are multiple representations of the body schema for the same body part. The body schema has been assumed to be a common body representation used to control all types of motor actions for more than a century (17, 19, 37–40). Although many studies have suggested that the body schema is based on the process of multisensory

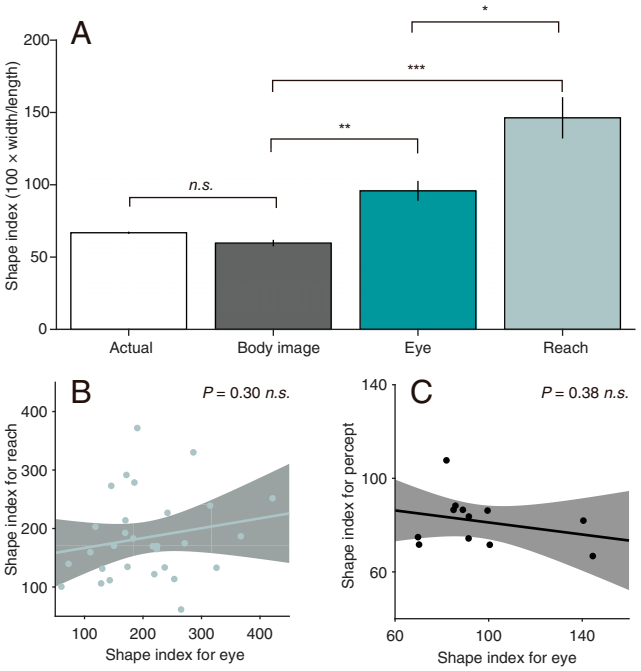

Fig. 5. Shape indices (100 × width/length) quantifying the overall aspect ratio of the hand. (*A*) Shape indices for the actual hand, the conscious body image measured by template matching, the body map measured by eye, and the body map measured by reach. Results are the mean ± SEM. (*B* and *C*) Regression plot (and 95% confidence bands) of shape indices. (*B*) Eye and reach movements without the CG hand. (*C*) Eye movements and perception with the CG hand. *$P < 0.05$; **$P < 0.01$; ***$P < 0.005$; *n.s.*: not significant.

integration (4–6, 17–20), I believe that the current systematic investigation of this process during multiple motor actions with different effectors is unique. The present results show that the body schema is organized as multiple effector-specific body representations. These representations were measured through proprioceptive judgments of body parts. These proprioceptive judgments show remarkably large distortions of the represented body shape, which are thought to reflect the characteristics of the body schema (12, 13, 61). I found that the pattern of the distortions differs between saccadic eye movements and reach movements even when these two types of movements are simultaneously directed to the same body part location. This difference was observed when an artificial body part spatially overlapped the participant's invisible body part but not when the artificial body part was replaced with a nonbody object. Moreover, the distortions of the represented body shape were not correlated between saccade and reach across individuals regardless of whether visual information about the artificial body part was available. These results provide clear evidence of a dissociation in body representations between different types of effectors and that these body representations differ in the weighting of visual and proprioceptive bodily cues.

What might be the mechanisms underlying such a dissociation in body representations between different types of effectors? Body representations are the spatial model of the body that the brain constructs based on the integration of information from multiple sensory modalities such as vision and proprioception (20, 62). Such body models can provide an estimate of where one's body parts are in space (12). This estimate is generated by combining bodily cues in a way that the weights change flexibly according to the uncertainty surrounding the body's location (31). For example, when vision is heavily weighted, an estimate of where one's body part is in space relies more on vision than on proprioception. Recent studies examining the integration of visual and proprioceptive bodily information suggest that the weighting of each bodily cue depends on its reliability (33, 35). However, the present results demonstrate that, even though the same visual and proprioceptive bodily cues are theoretically available for saccade and reach, these cues are incorporated differently for the two movements. Thus, this finding indicates that the weighting of vision and proprioception differs for each effector even though the reliability of each bodily cue is the same across the effectors being used.

The present results suggest that there are two distinct body representations for action. One body representation is used to guide saccadic eye movements, whereas the other is used to guide reach movements. Are these body representations different from a body representation for perception? Separate somatosensory processes have been proposed for perception and action (51). For example, illusory displacement of the perceived location of a participant's hidden hand toward a rubber hand presented in front of the participant, called proprioceptive drift, is reduced when tested with reach movements rather than perception (19). Consistent with this result, I found that the body representation for reach differed from that for perception. In contrast, the body representation for saccade was almost the same as that for perception. Furthermore, I found that the magnitude of the distortion of the body representation was significantly correlated with the strength of sense of body ownership over the CG hand for saccade and percept but not for reach. Although these results highlight the difference between the saccade and reach systems, the results indicate that both saccade and percept depend on a cross-modal effect of vision and proprioception on body ownership. However, I found that the distortions of the represented body shape were not correlated between saccade and percept across individuals. These findings suggest that dissociated processing of perception and action is a characteristic of both the saccade and reach systems.

The present results indicate that dissociable body representations are identified on motor tasks. Dissociation between body schema (a body representation used to control bodily movements) and body image (a body representation used to judge bodily properties) is well established (1, 4, 9). In the present study, participants controlled their saccade and reach movements toward their body parts. To carry out such motor tasks, the brain needs to have access to the body schema (1). For that reason, the body representations for saccade and reach should reflect the body schema. Indeed, I found that the body representations for saccade and reach are different from a conscious body image. These results suggest that the body representations for saccade and reach reflect the body schema and that the body schema can be further subdivided into at least two representations depending on the effector.

Which brain areas are responsible for the body representations for saccade and reach? Neuroimaging studies have suggested that the posterior parietal cortex (PPC), the ventral premotor cortex (PMV), and the extrastriate body area (EBA) are involved in the performance of motor actions (63–65). The PPC contains distinct cortical areas, the intraparietal sulcus (IPS) and the superior parietal lobe (SPL). The IPS and SPL are selectively recruited during saccade and reach movements, respectively (63). Like the PPC, the PMV also contains distinct cortical areas, the saccade-evoking area (PMVe) and the reach-evoking area (PMVr) (64). Like the SPL and PMVr, the EBA also responds during reach movements (65). Interestingly, the IPS, SPL, EBA, and PMV have also been suggested to be involved in the body representations (66, 67). The IPS and PMV have been reported to encode the hand position by integrating visual and proprioceptive signals (66, 68). Moreover, activity in the PMV reflects individual differences in experienced artificial hand ownership (67, 69). Unlike the IPS and PMV, the SPL and EBA have been found to encode changes in proprioceptive hand position in the dark, although these regions also responded to the position of a visible computer-generated hand (65, 67). These findings suggest that the contribution of vision and proprioception to the hand representation is different between the saccade-related IPS and PMVe and the reach-related SPL and EBA, although this contribution seems to be similar between the PMVe and the PMVr. This view is supported by the present results. Indeed, the present results indicate that the estimate of the landmark positions on the hand relies more heavily on proprioception for reach movements than for saccade movements. Taken together, these findings suggest that the IPS and PMVe may be responsible for the body representation accessed by the saccade system and that the SPL and EBA may be responsible for the body representation accessed by the reach system.

Although a common spatial representation in the brain is often believed to guide different types of effectors toward the same goal (49), some evidence suggests that different effectors aiming for the same goal can show different spatial representations. Visual motion processing is carried out independently for manual and ocular following responses to visual motion (41). The spatial localization of moving objects differs between eye and hand movements (42). During the preparation of coordinated eye–hand movements, spatial attention is allocated independently to the targets of both movements (43, 44). These previous studies propose the view that spatial maps of the outside world in the brain dissociate between different types of effectors. The present findings support this view and demonstrate that such dissociations are present not only with spatial maps of the outside world but also with spatial maps of one's body.

What are the different roles of the body representations accessed by the reach system and the saccade system? Distortions in hand representations have been reported to extend to objects (70). Interestingly, similar distortions to the hand representation were found for the representation of manipulable objects such as a mobile phone, but the pattern of distortions for nonmanipulable objects, such as a cactus with spines, differed from that for manipulable objects. This suggests that the pattern of distortions depends on the availability of motor functions. The present study indicates that this pattern of distortions also depends on the types of motor functions. Motor functions differ between reach and saccade. The reach system would allow us to interact with objects around us, whereas the saccade system would allow us to take advantage of foveal vision to judge whether our hands can safely interact with objects. I suggest that the body representations accessed by the reach system might be involved in facilitating body−object interactions, whereas those accessed by the saccade system might be less involved in manipulability of objects.

A visual distortion in HMDs is well established (71). However, this visual distortion in HMDs cannot explain the present results. The current study showed that there is a highly distorted representation of hand shape, shortened finger lengths, and wider hand widths using an HMD. If these results are due to the effects of the HMD, the results should be extended finger lengths and narrower hand widths (i.e., reversed) when the participant's hand and the CG hand are rotated 90° counterclockwise relative to their trunk (experiment 2). However, experiment 2 showed that the estimated finger lengths and hand widths in the rotated posture are almost identical to those in the original posture shown in experiment 1. This suggests that the present results are not due to the effects of the HMD itself. Nevertheless, because the CG hand leads to a misestimation of depth perception in a virtual 3D environment, it may be better to run a similar study using mixed reality in which participants see their real hand. Future research is needed to examine this topic.

The present study has implications for methods designed to visualize the body representations of patients with motor paralysis. The rapid population aging of many developed countries, such as Japan, will sharply increase the number of patients with motor paralysis resulting from motor dysfunction and stroke. To overcome this issue, effective rehabilitation techniques need to be developed for patients with motor paralysis. Visualization of the patient's body representations for action will help to build such an effective rehabilitation technique. The present results suggest that the choice of effectors toward one's body can determine which body representation in the brain is observed. This approach to the visualization of multiple body representations might be useful for understanding abnormal body schemas in patients with motor paralysis or limb amputation.

Materials and Methods

Participants. A total of 12 participants (five women and seven men; mean age, 22.42 [range, 19 to 24] y) were recruited in experiments 1, 2, and 4, whereas 18 participants (six women and 12 men; mean age, 22.0 [range, 19 to 25] y) were recruited in experiment 3. The same participants were tested in experiments 1 and 2. Participants were recruited from a paid participant pool (Sona Systems, Ltd.) and received a gift card of 1,000 yen per hour for their participation. This paid participant pool comprised individuals who wished to participate in research studies that were being conducted by Tohoku University faculty members and graduate students. Undergraduate and graduate students of Tohoku University were registered in the paid participant tool. All participants were naïve to the purpose of the experiments. They had normal or corrected-to-normal vision and provided informed consent in accordance with the Code of Ethics of the World Medical Association (Declaration of Helsinki). The study was approved by the Ethics Committee of the Graduate School of Information Sciences, Tohoku University. All methods were conducted in accordance with relevant guidelines and regulations. To confirm the necessary sample size, I conducted a power analysis that considers repetition of conditions (72). This power analysis was performed using a power analysis program, PANGEA (73), and revealed that the sample size should include ∼12 participants to obtain a statistical power of more than 0.80 for detecting a typical effect size (d = 0.75, Replicates = 40, and n = 12). This d was determined based on Cohen's definition (74). The conventional standard of the statistical power is thought to be 0.80 (75). For experiments 1, 2, and 4, the statistical power was 0.81 (d = 0.75, Replicates = 40, and n = 12). For experiment 3, the statistical power was 0.95 (d = 0.75, Replicates = 40, and n = 18).

Apparatus and Stimuli. Participants placed their right hand on a table and wore an HMD that displayed visual stimuli in stereoscopic 3D (76). A transparent board was placed over the hand, resting on two blocks (8 cm in height). The HMD was equipped with an eye tracker and a customized forehead rest. Reach movements were recorded with an electromagnetic tracking system. To photograph the participant's right hand, a camera was suspended above the center of the transparent board, pointing straight down. The participants viewed a realistic life-sized 3D CG hand (experiments 1 and 2) or a 3D wood-like rectangle (experiment 4) placed on a gray surface through the HMD, but they viewed the gray surface alone without the CG hand in experiment 3 (Fig. 1). The gray surface was spatially aligned with the real table (where the participants placed their hand). The participants were instructed to indicate the judged location of landmarks on their occluded right hand with their eyes and left index finger at the same time. A total of 10 landmarks were used: the knuckle at the base of each finger and the tip of each finger (the center of the fingernail). More details are given in *SI Appendix*.

Procedures. Each session started with an eye-movement calibration procedure. In each trial, a computer cued the participant as to which landmark to judge by using a prerecorded woman's voice. The participants were instructed to indicate the judged location of landmarks on their invisible right hand with both their eyes and left index finger at the same time (and not in turn). They were also instructed to make ballistic points with eye and reach. Before the start of each trial, the participants moved their gaze to a red dot near one of the four edges (randomly selected between the front, back, right, and left positions) of the gray surface in the virtual environment and moved the tip of their left index finger on a trackball placed to the left of the transparent board. The participants initiated a trial by pressing a button of the trackball using their left hand. After a randomly selected delay between 500 and 1,500 ms, the red dot was extinguished, which indicated the start of the trial, and the participants were instructed to make both eye and reach movements toward the landmark as soon as possible. The order of landmarks was counterbalanced across participants. Each condition comprised four sessions of 10 trials. Further information is given in *SI Appendix*.

Analysis.

Eye and hand movements. The landing position of eye and hand movements was defined as the initial movement end point. The movement end point was the position at which the offset of the movement was detected after the onset of the movement. The onset and offset of an eye were defined as the time at which eye velocity exceeded or fell below 30°/s, respectively. The onset and offset of a hand were defined as the time at which hand velocity exceeded or fell below 10°/s, respectively. More details are given in *SI Appendix*.

Data processing. The x–y centimeter coordinates of each landmark on the images of the actual hand and the corresponding eye and reach landing locations were coded using MATLAB. Mean coordinates were then calculated for each landmark. Distances were calculated between the tips and knuckles of each finger and between pairs of knuckles. More details are given in *SI Appendix*.

GPS. According to a previous study (12), GPS was used to compare the actual configuration of landmarks from each participant's hand with the internal representation based on localization judgments. GPS removes differences resulting from location, size, and orientation (55, 56) and was computed using MATLAB. To compare hand shapes, GPS analyses were conducted with CoordGen software, part of the Integrated Morphometrics Package Suite (77). More details are given in *SI Appendix*.

Data Availability. Anonymized raw data have been deposited in Open Science Framework (https://osf.io/cg8us/wiki/). All other study data are included in the article and/or *SI Appendix*.

ACKNOWLEDGMENTS. This work was partially supported by the Precursory Research for Embryonic Science and Technology, Japan Science and Technology (JPMJPR16DB), Japan Society for the Promotion of Science, Grants-in-Aid for Scientific Research (JP21361022), and a University–Industry Joint Research Project with Hitachi Ltd.

1. H. Head, G. Holmes, Sensory disturbances from cerebral lesions. *Brain* **34**, 102–254 (1911).
2. P. L. Strick, J. B. Preston, Multiple representation in the primate motor cortex. *Brain Res.* **154**, 366–370 (1978).
3. S. Gallagher, Body image and body schema: A conceptual clarification. *J. Mind Behav.* **7**, 541–554 (1986).
4. J. Bermúdez, A. Marcel, N. Eilan, *The Body and the Self* (The MIT Press, Cambridge, MA, 1995).
5. A. Maravita, C. Spence, J. Driver, Multisensory integration and the body schema: Close to hand and within reach. *Curr. Biol.* **13**, R531–R539 (2003).
6. S. Shokur *et al.*, Expanding the primate body schema in sensorimotor cortex by virtual touches of an avatar. *Proc. Natl. Acad. Sci. U.S.A.* **110**, 15121–15126 (2013).
7. P. Haggard, D. Wolpert, "Disorders of body scheme" in *Higher-Order Motor Disorders*, H.-J. Freund, Ed. (Oxford University Press, 2004), pp. 1–7.
8. J. Ota, E. Naito, N. Haga, *Embodied-Brain Systems Science and Rehabilitation Medicine, Motor Control* (The University of Tokyo Press, Tokyo, 2018).
9. J. Paillard, "Body schema and body image: A double dissociation in deafferented patients" in *Motor Control, Today and Tomorrow*, G. N. Gantchev, S. Mori, J. Massion, Eds. (Academia Press, 1999), pp. 197–214.
10. F. de Vignemont, Body schema and body image–Pros and cons. *Neuropsychologia* **48**, 669–680 (2010).
11. J. Medina, H. B. Coslett, From maps to form to space: Touch and the body schema. *Neuropsychologia* **48**, 645–654 (2010).
12. M. R. Longo, P. Haggard, An implicit body representation underlying human position sense. *Proc. Natl. Acad. Sci. U.S.A.* **107**, 11727–11732 (2010).
13. V. Peviani, G. Bottini, The distorted hand metric representation serves both perception and action. *J. Cogn. Psychol.* **30**, 880–893 (2018).
14. S. Gallagher, "Body schema and intentionality" in *The Body and the Self*, J. L. Bermudez, A. Marchel, N. Eilan, Eds. (The MIT Press, Cambridge, 1995), pp. 225–244.
15. J. P. Roll, R. Roll, "Kinaesthetic and motor effects of extraocular muscle vibration in man" in *Eye Movements: From Physiology to Cognition*, J. K. O'Regan, A. Levy-Schoen, Eds. (Elsevier Science Publishers, Amsterdam, 1987), pp. 57–68.
16. J. P. Roll, R. Roll, "From eye to foot: A proprioceptive chain involved in postural control" in *Posture and Gait: Development, Adaptation and Modulation*, G. Amblard, A. Berthoz, F. Clarac, Eds. (Excerpta Medica, Amsterdam, 1988), pp. 155–164.
17. A. Iriki, M. Tanaka, Y. Iwamura, Coding of modified body schema during tool use by macaque postcentral neurones. *Neuroreport* **7**, 2325–2330 (1996).
18. L. Cardinali, C. Brozzoli, A. Farnè, Peripersonal space and body schema: Two labels for the same concept? *Brain Topogr.* **21**, 252–260 (2009).
19. M. P. Kammers, F. de Vignemont, L. Verhagen, H. C. Dijkerman, The rubber hand illusion in action. *Neuropsychologia* **47**, 204–211 (2009).
20. M. Boccia *et al.*, Topological and hodological aspects of body representation in right brain damaged patients. *Neuropsychologia* **148**, 107637 (2020).
21. J. C. Hay, H. L. Pick, K. Ikeda, Visual capture produced by prism spectacles. *Psychon. Sci.* **2**, 215–216 (1965).
22. M. S. Graziano, Where is my arm? The relative role of vision and proprioception in the neuronal representation of limb position. *Proc. Natl. Acad. Sci. U.S.A.* **96**, 10418–10421 (1999).
23. F. Pavani, C. Spence, J. Driver, Visual capture of touch: Out-of-the-body experiences with rubber gloves. *Psychol. Sci.* **11**, 353–359 (2000).
24. M. Tsakiris, P. Haggard, The rubber hand illusion revisited: Visuotactile integration and self-attribution. *J. Exp. Psychol. Hum. Percept. Perform.* **31**, 80–91 (2005).
25. K. Matsumiya, S. Shioiri, Moving one's own body part induces a motion aftereffect anchored to the body part. *Curr. Biol.* **24**, 165–169 (2014).
26. K. Matsumiya, Awareness of voluntary action, rather than body ownership, improves motor control. *Sci. Rep.* **11**, 418 (2021).
27. M. S. A. Graziano, M. M. Botvinick, "How the brain represents the body: Insights from neurophysiology and psychology" in *Attention and Performance XIX*, W. Prinz, B. Hommel, Eds. (Oxford University Press, New York, 2002), pp. 136–157.
28. H. H. Ehrsson, "The concept of body ownership and its relation to multisensory integration" in *The New Handbook of Multisensory Processes*, B. E. Stein, Ed. (MIT Press, Cambridge, MA, 2012), pp. 775–792.
29. O. Blanke, Multisensory brain mechanisms of bodily self-consciousness. *Nat. Rev. Neurosci.* **13**, 556–571 (2012).
30. M. O. Ernst, M. S. Banks, Humans integrate visual and haptic information in a statistically optimal fashion. *Nature* **415**, 429–433 (2002).
31. R. J. van Beers, D. M. Wolpert, P. Haggard, When feeling is more important than seeing in sensorimotor adaptation. *Curr. Biol.* **12**, 834–837 (2002).
32. D. Alais, D. Burr, The ventriloquist effect results from near-optimal bimodal integration. *Curr. Biol.* **14**, 257–262 (2004).
33. M. Samad, A. J. Chung, L. Shams, Perception of body ownership is driven by Bayesian sensory inference. *PLoS One* **10**, e0117178 (2015).
34. J. P. Noel, O. Blanke, A. Serino, From multisensory integration in peripersonal space to bodily self-consciousness: From statistical regularities to statistical inference. *Ann. N. Y. Acad. Sci.* 10.1111/nyas.13867. (2018).
35. K. Matsumiya, Separate multisensory integration processes for ownership and localization of body parts. *Sci. Rep.* **9**, 652 (2019).
36. M. Botvinick, J. Cohen, Rubber hands 'feel' touch that eyes see. *Nature* **391**, 756 (1998).
37. R. Romo, E. Salinas, Sensing and deciding in the somatosensory system. *Curr. Opin. Neurobiol.* **9**, 487–493 (1999).
38. N. P. Holmes, H. J. Snijders, C. Spence, Reaching with alien limbs: Visual exposure to prosthetic hands in a mirror biases proprioception without accompanying illusions of ownership. *Percept. Psychophys.* **68**, 685–701 (2006).
39. L. Cardinali *et al.*, Tool-use induces morphological updating of the body schema. *Curr. Biol.* **19**, R478–R479 (2009).
40. R. Newport, R. Pearce, C. Preston, Fake hands in action: Embodiment and control of supernumerary limbs. *Exp. Brain Res.* **204**, 385–395 (2010).
41. H. Gomi, N. Abekawa, S. Shimojo, The hand sees visual periphery better than the eye: Motor-dependent visual motion analyses. *J. Neurosci.* **33**, 16502–16509 (2013).
42. M. Lisi, P. Cavanagh, Different spatial representations guide eye and hand movements. *J. Vis.* **17**, 12 (2017).
43. D. Jonikaitis, H. Deubel, Independent allocation of attention to eye and hand targets in coordinated eye-hand movements. *Psychol. Sci.* **22**, 339–347 (2011).
44. N. M. Hanning, D. Aagten-Murphy, H. Deubel, Independent selection of eye and hand targets suggests effector-specific attentional mechanisms. *Sci. Rep.* **8**, 9434 (2018).
45. O. Bock, Contribution of retinal versus extraretinal signals towards visual localization in goal-directed movements. *Exp. Brain Res.* **64**, 476–482 (1986).
46. J. T. Enright, The non-visual impact of eye orientation on eye-hand coordination. *Vision Res.* **35**, 1611–1618 (1995).
47. D. Y. Henriques, E. M. Klier, M. A. Smith, D. Lowy, J. D. Crawford, Gaze-centered remapping of remembered visual space in an open-loop pointing task. *J. Neurosci.* **18**, 1583–1594 (1998).
48. A. P. Batista, C. A. Buneo, L. H. Snyder, R. A. Andersen, Reach plans in eye-centered coordinates. *Science* **285**, 257–260 (1999).
49. Y. E. Cohen, R. A. Andersen, A common reference frame for movement plans in the posterior parietal cortex. *Nat. Rev. Neurosci.* **3**, 553–562 (2002).
50. A. Pouget, J. C. Ducom, J. Torri, D. Bavelier, Multisensory spatial representations in eye-centered coordinates for reaching. *Cognition* **83**, B1–B11 (2002).
51. H. C. Dijkerman, E. H. de Haan, Somatosensory processes subserving perception and action. *Behav. Brain Sci.* **30**, 189–201 (2007).
52. C. Prablanc, J. E. Echallier, M. Jeannerod, E. Komilis, Optimal response of eye and hand motor systems in pointing at a visual target. II. Static and dynamic visual cues in the control of hand movement. *Biol. Cybern.* **35**, 183–187 (1979).
53. M. Land, N. Mennie, J. Rusted, The roles of vision and eye movements in the control of activities of daily living. *Perception* **28**, 1311–1328 (1999).
54. R. S. Johansson, G. Westling, A. Bäckström, J. R. Flanagan, Eye-hand coordination in object manipulation. *J. Neurosci.* **21**, 6917–6932 (2001).
55. F. J. Rohlf, D. E. Slice, Extensions of the procrustes method for the optimal superimposition of landmarks. *Syst. Zool.* **39**, 40–59 (1990).
56. F. L. Bookstein, *Morphometric Tools for Landmark Data: Geometry and Biology* (Cambridge University Press, Cambridge, 1991).
57. M. Slater, D. Perez-Marcos, H. H. Ehrsson, M. V. Sanchez-Vives, Inducing illusory ownership of a virtual body. *Front. Neurosci.* **3**, 214–220 (2009).
58. J. Napier, *Hands* (Princeton University Press, Princeton, NJ, 1980).
59. M. R. Longo, F. Schüür, M. P. Kammers, M. Tsakiris, P. Haggard, Self awareness and the body image. *Acta Psychol. (Amst.)* **132**, 166–172 (2009).
60. J. B. Wilmer, K. Nakayama, Two distinct visual motion mechanisms for smooth pursuit: Evidence from individual differences. *Neuron* **54**, 987–1000 (2007).
61. M. R. Longo, Implicit and explicit body representations. *Eur. Psychol.* **20**, 6–15 (2015).
62. J. Schwoebel, H. B. Coslett, Evidence for multiple, distinct representations of the human body. *J. Cogn. Neurosci.* **17**, 543–553 (2005).
63. S. V. Astafiev *et al.*, Functional organization of human intraparietal and frontal cortex for attending, looking, and pointing. *J. Neurosci.* **23**, 4689–4699 (2003).
64. N. Fujii, H. Mushiake, J. Tanji, An oculomotor representation area within the ventral premotor cortex. *Proc. Natl. Acad. Sci. U.S.A.* **95**, 12034–12037 (1998).
65. S. V. Astafiev, C. M. Stanley, G. L. Shulman, M. Corbetta, Extrastriate body area in human occipital cortex responds to the performance of motor actions. *Nat. Neurosci.* **7**, 542–548 (2004).
66. C. Brozzoli, G. Gentile, H. H. Ehrsson, That's near my hand! Parietal and premotor coding of hand-centered space contributes to localization and self-attribution of the hand. *J. Neurosci.* **32**, 14573–14582 (2012).
67. J. Limanowski, F. Blankenburg, Integration of visual and proprioceptive limb position information in human posterior parietal, premotor, and extrastriate cortex. *J. Neurosci.* **36**, 2582–2589 (2016).
68. D. M. Lloyd, D. I. Shore, C. Spence, G. A. Calvert, Multisensory representation of limb position in human premotor cortex. *Nat. Neurosci.* **6**, 17–18 (2003).
69. H. H. Ehrsson, C. Spence, R. E. Passingham, That's my hand! Activity in premotor cortex reflects feeling of ownership of a limb. *Science* **305**, 875–877 (2004).
70. V. Peviani, F. G. Magnani, G. Bottini, L. Melloni, Metric biases in body representation extend to objects. *Cognition* **206**, 104490 (2021).
71. F. El Jamiy, R. Marsh, Survey on depth perception in head mounted displays: Distance estimation in virtual reality, augmented reality, and mixed reality. *IET Image Process.* **15**, 707–712 (2019).

72. J. Westfall, D. A. Kenny, C. M. Judd, Statistical power and optimal design in experiments in which samples of participants respond to samples of stimuli. *J. Exp. Psychol. Gen.* **143**, 2020–2045 (2014).
73. H. Singmann, D. Kellen, "An introduction to mixed models for experimental psychology" in *New Methods in Cognitive Psychology*, D. Spieler, E. Schumacher, Eds. (Routledge, New York, 2019), pp. 4–31.
74. J. Cohen, A power primer. *Psychol. Bull.* **112**, 155–159 (1992).
75. J. Cohen, *Statistical Power Analysis for the Behavioral Sciences* (Erlbaum, Hillsdale, NJ, ed. 2, 1988).
76. R. Tachibana, K. Matsumiya, Accuracy and precision of visual and auditory stimulus presentation in virtual reality in Python 2 and 3 environments for human behavior research. *Behav. Res. Methods*, 10.3758/s13428-021-01663-w (2021).
77. H. D. Sheets, Integrated morphometrics package (IMP) 8 (2014). https://www.animalbehaviour.de/imp/. Accessed 12 January 2022.